Core-rim structure formation in TiC-Ni based cermets fabricated by a combined thermal explosion/hot-pressing process

S. Lemboub, S. Boudebane, F.J. Gotor, S. Haouli, S. Mezrag, S. Bouhedja, G. Hesser, H. Chadli, T. Chouchane

PII: S0263-4368(17)30515-2
DOI: doi:10.1016/j.ijrmhm.2017.09.014
Reference: RMHM 4523

To appear in: *International Journal of Refractory Metals and Hard Materials*

Received date: 3 August 2017
Revised date: 16 September 2017
Accepted date: 21 September 2017

Please cite this article as: S. Lemboub, S. Boudebane, F.J. Gotor, S. Haouli, S. Mezrag, S. Bouhedja, G. Hesser, H. Chadli, T. Chouchane , Core-rim structure formation in TiC-Ni based cermets fabricated by a combined thermal explosion/hot-pressing process. The address for the corresponding author was captured as affiliation for all authors. Please check if appropriate. Rmhm(2017), doi:10.1016/j.ijrmhm.2017.09.014

Core-rim structure formation in TiC-Ni based cermets fabricated by a combined thermal explosion/hot-pressing process

S. Lemboub[a b*], S. Boudebane[a], F.J. Gotor[c], S. Haouli[a], S. Mezrag[a], S. Bouhedja[d], G. Hesser[e]
H. Chadli [b], T. Chouchane[f]

[a]*Département et Laboratoire de Métallurgie et Génie des Matériaux, Faculté des sciences de l'ingéniorat Université Badji Mokhtar-Annaba, BP 12 Annaba 23000, Algeria.*

[b]*Ecole Nationale Supérieure des Mines et Métallurgie-Annaba BP 233 RP Annaba 23000, Algeria.*

[c]*Instituto de Ciencia de Materiales de Sevilla (CSIC-US), 41092 Sevilla, Spain.*

[d]*Laboratoire des hyperfréquences et semi-conducteurs, Faculté des sciences et technologie, Université des frères Mentouri – BP 325, Constantine 25017, Algeria.*

[e]*IUT d'Orsay rue Noetzlin Plateau de Moulon, Orsay 91400, France.*

[f]*Research Center in Industrial Technologies CRTI, P.O. Box 64, Cheraga 16014 Algiers, Algeria.*

**Corresponding author –"lemboubs@yahoo.fr"*

Abstract

TiC-Ni-based cermets were obtained by thermal explosion from different elemental mixtures (Ti, C, Ni and X, where X = Cr, Mo or W) and subsequently densified by hot-pressing under a cyclic load. The whole process was performed in a single stage in the same experimental device according to the following thermal and pressure procedure: a heating rate ramp up to 1573 K without applying any load followed by an isothermal dwelling under a compressive cyclic load of 32 MPa. The thermal explosion synthesis occurred during the heating ramp at a temperature close to 1273 K that was practically independent of the starting nominal composition. The influence of different refractory elements on the chemical composition and microstructure of cermets was studied. SEM characterization showed that only with Mo and W, the cermets developed the characteristic core-rim structure. A high densification was achieved, but decreased when the refractory elements were added. Nevertheless, in these cases higher hardness values were obtained.

Keywords: Cermets, Thermal explosion, Core-rim microstructure, Solid-solution carbides

1. Introduction

Cermets based on TiC-Ni, (Ti, W)C-Ni, (Ti, Mo)C-Ni and Ti(C, N)-Ni have received increasing attention [1, 2] in recent years because of their extreme hardness, high wear resistance, high-temperature stability and chemical inertness [3-5]. Cermets are particularly suitable as materials for cutting tools and are commonly produced following a powder metallurgy method. The manufacturing process generally includes a sintering step in the presence of a permanent liquid phase (molten binder) [6], during which cermets acquire the characteristic core-rim structure [7].

Several works on liquid phase sintering of TiC-Ni- and Ti(C, N)-Ni-based cermets agree that the formation of the core-rim structure occurs according to a dissolution-reprecipitation mechanism [7-10]. In this case, the dissolution of TiC or Ti(C, N) ceramic particles in the liquid phase together with other secondary carbides, such as Mo_2C, WC, TaC or NbC, which are added to modulate the microstructure and mechanical properties of cermets, is accompanied by the reprecipitation of a complex carbide or carbonitride (rim) on the undissolved TiC or Ti(C, N) particles (core). Therefore, the formation mechanism of the core-rim structure is conditioned by the presence of a permanent liquid phase during sintering and a cermets' starting composition that favors the appearance of this particular microstructure. Some studies suggest that the appearance of the core-rim structure starts with the formation of an inner-rim with a thickness of a few nanometers caused by a solid state diffusion process and ends with the formation of a second outer-rim by the mentioned dissolution-reprecipitation mechanism [11-13].

Although comprehensive knowledge of the core-rim structure obtained by liquid phase sintering has been acquired, opinions on the influence of this specific structure on the cermets properties are not always convergent. Thereby, it appears that the rim phase improves the wettability of the hard phase with the binder phase and would inhibit the approach of Ti(C, N)

particles to each other, hindering the coarsening of the Ti(C, N) grains. As mentioned in reference [14], a much complete rim phase would strengthen the cohesion between the ceramic and binder phases, preventing the crack propagation in cermets. However, according to these same authors, the strength of the cermets would tend to decrease sharply when the rim thickness is larger than 0.5 μm. Some others authors have claimed conversely that a significant degradation of the cermet toughness can be caused by the formation of the interface between the core and the rim that generates residual stresses that accelerate the crack propagation [15]. Radjabi and al. [16] have drawn attention in the stress state of the core-rim structure and consider that increasing the rim thickness leads to the toughness decreasing of cermets due to the development of tensile stresses at the core-rim interface.

By other hand, as TiC and Ti(C, N), as well as other transition metal carbides, can be produced by combustion processes [17], many researchers have applied this methodology in the development of cermets. The self-propagating high-temperature synthesis (SHS) method has been more widely employed [18-20] compared with the thermal explosion (TE) method [21]. The difference between the two combustion modes is that in SHS only one end of the reactant compact is ignited, while in TE, ignition occurs in the whole compact. The activated combustion by high energy milling, called mechanically induced self-sustaining reaction (MSR), has also been proposed to produce novel cermets compositions [22, 23].

Recently, new procedures combining combustion (SHS or TE) and pressing methods have been developed to perform a one-step synthesis/densification process [24-26]. In these processes, a uniaxial load is applied just after the combustion reaction is produced. Note that the main advantage of the proposed regime is to substantially shorten the overall cycle of the cermets production. Until now, simple gross compositions, usually Ti-C-Ni blends have been explored with practically no works dealing with more complex mixtures, especially if they contain transition metals that are prone to induce the formation of the core-rim structure. In

these cases, the core-rim structure may also appear, but according to a relatively different mechanism compared to that observed during conventional liquid-phase sintering, as the liquid phase can be in this case transient and disappear some time after the extinction of the combustion wave.

In this context, the present work aims to study in detail the microstructure of TiC-Ni based cermets fabricated by a coupled procedure, combining combustion in a thermal explosion mode and hot-pressing, from elemental mixtures containing Ti, C, Ni and also Cr, Mo or W additions. Special attention was paid to the evolution of the core-rim structure during the fabrication process.

2-Experimental procedure

The characteristics of the raw powders are shown in Table 1.

Table 1. Characteristics of starting powders.

Powder	Particle size (µm)	Purity (%)	Supplier
Ti	< 44	99.5	Aldrich
Cr	< 44	99.0	Alfa Aesar
Mo	2	99.9	Good Fellow
W	100	99.95	Good Fellow
Ni	3-7	99.9	Alfa Aesar
Graphite	1-2	-	Aldrich

The starting and final targeted compositions of the cermets are presented in Table 2.

Table 2. Starting powder mixtures and targeted final composition of studied cermets.

Sample.	Initial composition of powders mixtures (%wt.)	Cermets targeted composition (%wt.)
S_0	70(80Ti+20C)+30Ni	70TiC + 30Ni
S_1	70[80(80Ti+20C)+20(86.67Cr+13.33C)]+30Ni	70(80TiC+20Cr_3C_2)+30Ni
S_2	70[80(80Ti+20C)+20(94.12Mo+5.88C)]+30Ni	70(80TiC+20Mo_2C)+30Ni
S_3	70[80(80Ti+20C)+20(93.9W+6.1C)]+30Ni	70(80TiC+20WC)+30Ni

The initial powders were first mixed by ball milling for 21.6 ks using stainless steel balls and then dried in an oven at 363 K for 86.4 ks to remove moisture. Pellets 30 mm in diameter with a weight of 5 g were compacted in a tungsten carbide die to achieve a green density of approximately 50%.

The green compact was introduced in a graphite die and positioned in the hot press device (model FCT 2000-50). The samples were heated at a rate of 5.2 K/s up to 1573 K in a primary vacuum without applying any load, followed by a 3.6 ks isothermal dwell under a cyclic load of 32 MPa. The samples were cooled at a rate of 4.7 K/s. A cyclic load (0.3 ks) was used to reduce the metal binder losses between die and punch by viscous flow and improve the final density of cermets. This whole process was called as TE + HP procedure. For a comparative purpose, some samples were also prepared by applying the compressive load during both the heating step and the isothermal dwelling (TE/HP procedure) or simply by thermal explosion without isothermal dwelling and load (TE procedure). Figure 1 shows a schematic of the special assembly implemented in addition to the temperature and load profiles used in the TE + HP procedure.

Figure 1. Temperature and cyclic load profiles (a), schematic of the combined thermal explosion-pressing device (b).

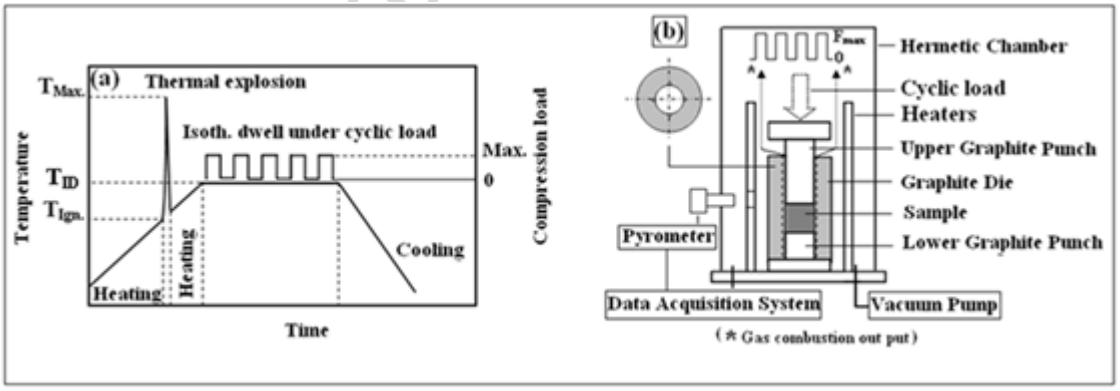

X-ray diffraction (XRD) diagrams were performed on a Panalytical X 'Pert Highscore diffractometer using Cu Kα radiation. The lattice parameter "*a*" of the TiC cubic phase was calculated from the position of the diffraction peaks (111), (200), (220) and (311). The Williamson Hall method [27] was used to separate the individual contributions of the crystallite size and lattice micro-strain on the XRD peak broadening.

Scanning electron microscopy (SEM) and energy-dispersive X-ray spectroscopy (EDS) were realized using Philips XL30 and FEI Quanta-250 microscopes. Specimens for microscopic examinations were polished and then cleaned by immersion in ultrasonic bath for 3.6 ks to remove any trace of impurities adhered to the surface of the sample.

The green density of the cold pre-compacted material was determined based on sample weight and volume measurements. However, the density of the densified cermets (d_m) was obtained by the Archimedes method. The relative density of cermets was estimated in accordance with the theoretical density (d_{th}) calculated by the rule of mixtures. The Vickers hardness measurements (HV) were carried out using an Innovatest 400 model durometer with a load of 0.2 kgf.

3. Results and discussion

3.1 The manufacturing process

The combustion synthesis in the thermal explosion mode occurred during the heating step when the ignition temperature ($T_{ign.}$) of the exothermic reaction of the TiC formation (ΔH_{f298K} = -184.3 kJ/mol [28]) was reached. This temperature was determined accurately because a sharp peak appeared in the record of the monitored pressure inside the reactor as a result of the heat release and the evaporation of volatile species. Due to the reaction heat, the sample temperature reached its maximum value ($T_{max.}$) just after ignition and before attaining the isothermal regime (Fig. 1(a)). In a previous work using a TE + HP procedure and similar experimental conditions [24], it was experimentally demonstrated that the sample temperature after the thermal explosion reached again the programmed temperature profile of the furnace after a short period of time. Therefore, in the present case, although it was not possible to directly measure the sample temperature, it was assumed that this temperature was effectively 1573 K during the isothermal dwelling as shown in Figure 1(a). In combustion processes,

$T_{max.}$ is always lower than the adiabatic temperature ($T_{ad.}$) as a result of heat losses. However, as in our case the whole sample is being heated, these losses are reduced and T_{ad} values can be taken as an upper limit not too far from the actual $T_{max.}$ values. Using the method developed by B. Holt and Z. A. Munir [29], the $T_{ad.}$ values for the different samples were calculated. Table 3 presents the thermal explosion results and the experimental conditions used during the fabrication of the different cermets.

It should be noted that the thermal explosion parameters, $T_{ign.}$ and T_{ad} (Table 3), depended on the nature of the additions and compositions of the starting mixtures. T_{ad} for the

Table 3. Experimental conditions and thermal explosion results.

Sample	Starting mixture (%wt.)	Applied regime	Thermal Explosion (TE)		Hot Pressing (HP)		
			$T_{ign.}$* (K)	$T_{ad.}$** (K)	Temp. (K)	Isot. Hold. (ks)	Cyclic Load (MPa)
S_0	70(Ti + C) +30Ni	TE + HP	1281	2546	1573	3.6	32
S'_0	70(Ti + C) +30Ni	TE	1281	2546	-	-	-
S_1	70(Ti + C + Cr) +30Ni	TE + HP	1273	2410	1573	3.6	32
S'_1	70(Ti + C + Cr) +30Ni	TE	1273	2410	-	-	-
S_2	70(Ti + C + Mo)+30Ni	TE + HP	1271	2330	1573	3.6	32
S'_2	70(Ti + C + Mo)+30Ni	TE	1271	2330	-	-	-
S_3	70(Ti + C + W) +30Ni	TE + HP	1268	2223	1573	3.6	32
S'_3	70(Ti + C + W) +30Ni	TE	1268	2223	-	-	-
S_{01}	70(Ti + C) +30Ni	TE/HP	1281	2551	1573	3.6	32
S_{03}	90(Ti + C) +10Ni	TE + HP	1353	3047	1573	3.6	32
S_{04}	60(Ti + C) +40Ni	TE + HP	1271	2272	1573	3.6	32

(TE+HP): (Thermal Explosion + Hot Pressing), (TE/HP: Combined), (HP: Hot Pressing); * Measured, ** Calculated

TiC synthesis is greater than 3273 K [29], but it decreases significantly when Ni is introduced into the starting mixture because it acts as a diluent and thus part of the released heat is consumed by the binder melting. For S_{03} sample, containing only 10 wt.% Ni, T_{ad} is reduced to 3047 K. As the amount of Ni in the mixture increases, T_{ad} is further reduced and values of 2546 K and 2272 K were calculated for cermets S_0 and S_{04} with 30 and 40 wt.% Ni, respectively. The addition of the refractory elements (Cr, Mo or W) also influences the heat balance of the TiC reaction synthesis by the possible formation of secondary carbides, such as

Cr_3C_2, Mo_2C and WC. When Cr is added to the Ti-C-Ni mixture with 30 wt.% Ni (S_1 cermet), T_{ad} decreases slightly from 2546 K to 2410 K. In the presence of Mo (S_2 cermet), T_{ad} decreases further to 2330 K. The lowest T_{ad} (2223 K) was obtained in samples with W addition (S_3 cermet).

Table 3 shows that the influence of the starting composition on $T_{ign.}$ was much lower than for $T_{ad.}$. This behavior is because $T_{ign.}$ is mainly conditioned by the appearance of a liquid phase at 1215 K corresponding to the Ti$_\beta$-$NiTi_2$ eutectic in the Ti-Ni system. It has been shown in previous studies that C particles begin to dissolve in this Ti–Ni liquid phase, which leads to the nucleation of the first TiC particles, releasing enough heat to trigger the ignition of the combustion process [18, 24]. Table 3 further shows that $T_{ign.}$ is slightly reduced with Cr, Mo or W additions, probably because the presence of these metals induced the appearance of the first liquid phase at a lower temperature. It was also observed that $T_{ign.}$ was more influenced by the Ni content. For cermets containing 10 wt.%Ni (S_{03}), the measured $T_{ign.}$ value was 1353 K, while when the metal binder content was increased up to 40wt.% (S_{04}), $T_{ign.}$ was reduced to 1271 K. This fact was the consequence of the formation of a greater proportion of liquid phase when increasing the Ni content, favoring the nucleation and precipitation of the first TiC particles above mentioned.

The highest relative density (96%) was obtained for the basic S_0 cermet, containing TiC+30 wt.%Ni without any addition, from the TE + HP procedure (Table 4).

Table 4. TiC particle size, relative density and Hardness values as a function of cermets composition and applied regime.

Sample	Applied regime	Average TiC particle size (μm)	Porosity (%)	Relative density (%)	Hardness $HV_{0.2}$ (MPa)
S_0	TE + HP	1.92	4	96	11590 ± 1050
S_1	TE + HP	4.65	5	95	15110 ± 1161
S_2	TE + HP	1.70	10	90	18000 ± 1820
S_3	TE + HP	2.84	7	93	16320 ± 790
S_{01}	TE/HP	-	14	86	-
S_{03}	TE + HP	-	42	58	-

However, when a load was applied during the thermal explosion, TE/HP procedure, the cermet density (S_{01} sample) achieved was relatively low (86%). Several phenomena causing the porosity in materials fabricated from combustion processes have been well elucidated in previous works [30]. It has been shown that the propagation of the combustion front in SHS processes is always accompanied by an increase in pressure due to the impurities burn-off and the partial evaporation of the starting constituents. These observations remain also valid in the case of combustion in the thermal explosion mode. Note that it is thanks to this pressure increase that it was possible to detect the ignition in the present work. The application of load during the thermal explosion in the TE/HP procedure hinders the escape of these gaseous species leading to a final low density and the presence of porosity in cermets.

By other hand, it was observed that the reduction of the binder content negatively affected the relative density of cermets, which did not exceed 58% when the Ni amount was only 10 wt.% (S_{03} cermet). Moreover, the addition of Cr, Mo or W also had a detrimental impact on the relative density of cermets. The residual porosity values observed for these cermets (S_1, S_2 and S_3 cermet) varied in the range of 5 to 10% (Table 4). Despite this lower density, the Vickers hardness of cermets with Cr, Mo or W additions was substantially higher (Table 4). The maximum hardness value was 18000 MPa for S_2 sample containing Mo. The hardness values of S_1 and S_3 samples with Cr and W were 15110 and 16320 MPa, respectively, still considerably higher than that of S_0 sample (11590 MPa).

Figure 2 shows the XRD patterns of S'_0, S'_1, S'_2 and S'_3 cermets obtained by TE (without isothermal dwelling and load) and S_0, S_1, S_2 and S_3 cermets elaborated through the TE + HP procedure. The XRD pattern of the S'_0 sample, with the basic composition 70(80Ti + 20C) + 30Ni, revealed the presence of TiC and Ni, but also free carbon was observed, indicating an incomplete combustion synthesis. A slight shift was evidenced in Ni peaks, probably due to the presence of a small amount of Ti dissolved in the Ni structure. TiC and Ni

phases were also identified in S_0 sample with the same composition as S'_0. Small free graphite peaks persisted because the dwelling time at 1573 K may be insufficient to ensure a complete dissolution. During this isothermal dwelling, most of the unreacted graphite dissolved and migrated through the metallic binder to the TiC–Ni boundary, diffusing through the interface and thus causing the increase of the C/Ti ratio in TiC. Also, this C reacts with Ti still present in the binder, avoiding the formation of intermetallic phases after cooling.

When the Cr is added to the basic mixture, the TiC synthesis is accompanied by the formation of $Cr_{23}C_6$, as shown in the XRD pattern of S'_1 sample obtained by TE (Fig. 2). Also

Figure 2. XRD patterns of S'_0, S'_1, S'_2 and S'_3 samples after the TE procedure and S_0, S_1, S_2 and S_3 samples after the TE + HP procedure.

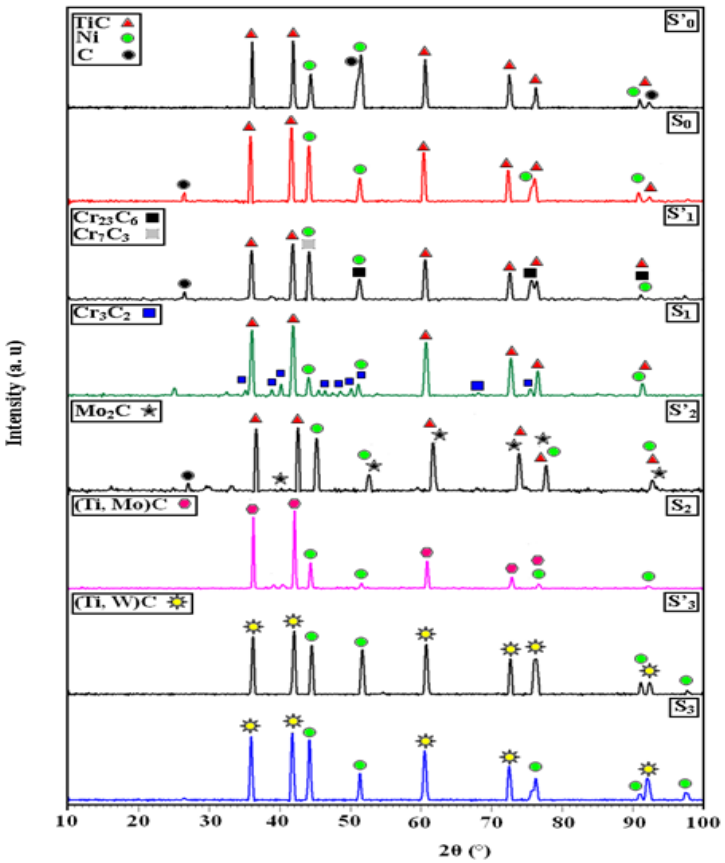

in this case, Ni and unreacted graphite were observed. Concerning S_1 sample prepared according to the complete regime, i.e. TE + HP, the XRD analysis revealed the presence of

TiC and Cr_3C_2. In this case, again as detailed above, the isothermal dwelling step led to the dissolution of the residual graphite in the metal binder, which justifies the appearance of a chromium carbide phase richer in carbon.

The TE process of the Mo containing mixture (S'_2) resulted in the synthesis of TiC and Mo_2C, as proven by the XRD pattern (Fig. 2) that show the presence of these carbides together with Ni and free C. Molybdenum carbide was formed during the exothermic peak of the thermal explosion process despite its low enthalpy (ΔH_{f298K} = -45.6 kJ/mol) [15]. The synthesis reaction was strongly activated by excess surface energy of small Mo particle size (Table 1). When this composition (S_2) was subjected to the TE + HP procedure, a shift in the position of TiC peaks was observed, which suggests the conversion of Mo_2C in MoC to form a complex (Ti, Mo)C solid solution (Fig. 2**).**

The XRD results of S'_3 sample with W confirmed the appearance of mixed carbide (Ti, W)C resulting from the interaction between TiC and WC, which were synthesized simultaneously during the thermal explosion process. This complex carbide is therefore obtained directly after the exothermic peak without formation of W_2C secondary carbide. In this case, the isothermal dwelling will lead only to the W enrichment of the mixed carbide (Ti, W)C and the formation of a more complex core rim structure (S_3 sample).

Considering that the formation of mixed carbides leads to changes in the lattice parameter (*a*) of the TiC-based cubic structure, an evaluation of this crystallographic parameter was undertaken from the XRD results (Fig. 3). Table 5 illustrates the variations of this parameter as a function of the applied regime and the nature of additions in the starting mixture. It appears that the parameter values after the TE process (S' samples) always remained below the theoretical value of TiC (4.328 Å) [28]. It is well-known that TiC is a

Figure 3. Williamson-Hall plots obtained on S'_3 and S_3 samples.

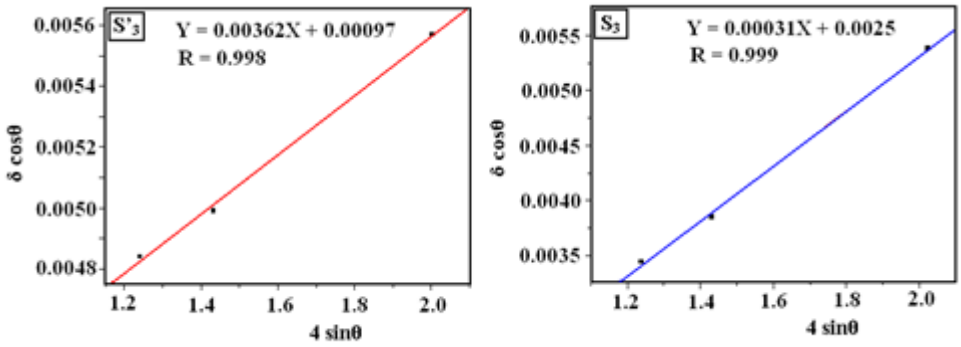

Table 5. TiC lattice parameter and micro-strain values as a function of cermets composition and applied regime.

Sample	Applied regime	TiC lattice parameter (Å)	Micro-strain (ε) x 10^{-4} (%)
S'_0	Thermal Explosion (TE)	4.31823	+7.58
S_0	Thermal Explosion + High Pressing (TE + HP)	4.33823	+4.93
S'_1	TE	4.32524	+31.1
S_1	(TE + HP)	4.32262	+14.4
S'_2	TE	4.31986	+20.8
S_2	(TE + HP)	4.31696	+13.1
S'_3	TE	4.32448	+36.2
S_3	(TE + HP)	4.31461	+3.11
Ref. [28]	-	4.32800	

non-stoichiometric compound with an extended homogeneity interval [31] and the lattice parameter decreases with decreasing carbon stoichiometry. It is then possible that the rapid combustion process produced a non-stoichiometric phase. Note that the XRD patterns of these samples presented frequently unreacted C. An increase of the lattice parameter was observed for S_0 subjected to the TE + HP procedure when compared to S'_0 without isothermal dwelling (Table 5). This effect was due to the incorporation of the unreacted C to the TiC-based lattice during the isothermal dwelling stage, increasing the C/Me ratio in the structure.

The differences observed in the lattice parameter of cermets containing refractory metal additives may also be related to the formation of mixed carbides, particularly with Mo and W additions, and the presence of secondary carbide phases, such as $Cr_{23}C_6$ and Mo_2C

(Fig. 2), which extract C from the reactant mixture. Moreover, the existence of a higher proportion of Mo and W in the mixed carbide in samples S_2 and S_3, respectively, may also modify the lattice parameters. After the TE + HP procedure, a decrease of TiC lattice parameter was observed in S_2 and S_3 cermets compared to the samples S'_2 and S'_3 (Table 5). The substitution of Ti atoms by refractory metals to form mixed carbides (Ti, Mo)C or (Ti, W)C leads to a slight contraction due to the difference in the atomic radius of Mo (0.1386 nm) and W (0.1394 nm) relatively to Ti atom (0.1467 nm) [28]. On the other hand, when Cr is added to the basic mixture, the formation of secondary chromium carbides was observed, and in this case the TiC lattice parameter remained practically constant independently of the applied regime (S'_1 and S_1 samples) (Table 5).

Since the substitution of Mo and W in the TiC-based lattice can generate distortions in the material structure, the stress state was also determined using the Williamson Hall method from the XRD results (Fig. 3). In our case, the stress state can also be affected by the applied regime during synthesis. Thus, after the thermal explosion, the stress induced in TiC particles is higher compared to that generated through the whole TE + HP process (Table 5). Thus after combustion, the stress is more intense in all samples which can be explained by the brutal character of the thermal explosion process governing the TiC particle synthesis. This stress state is more developed in the case of S'_2 and S'_3 cermets, containing Mo or W respectively. In addition, the formation of mixed carbides (Ti, Mo)C or (Ti, W)C after the isothermal dwelling (S_2 and S_3 samples) leads to the decreasing in the titanium carbide lattice parameter and consequently the lowering of the micro-strains level (Table 5).

3.2. Microstructure of cermets

Under our experimental conditions, the formation of the cermets' structure, regardless of the composition, begins with the thermal explosion process, since the samples reach the maximum temperature after ignition, and continues during the isothermal dwelling at 1573 K.

Note that the melting point of the binary eutectic reaction in the TiC–Ni system has been determined as 1568 K [6] and it can be assumed then that the presence of a liquid phase, even in a small amount, exists during the isothermal dwelling at 1573 K.

Figure (4a) shows the backscattered electron micrograph of the S_0 sample with the basic composition. The microstructure comprises spherical TiC particles with a mean

Figure 4. SEM micrographs of polished specimens S_0 (a), S_{01} (b) and S_1 (c).

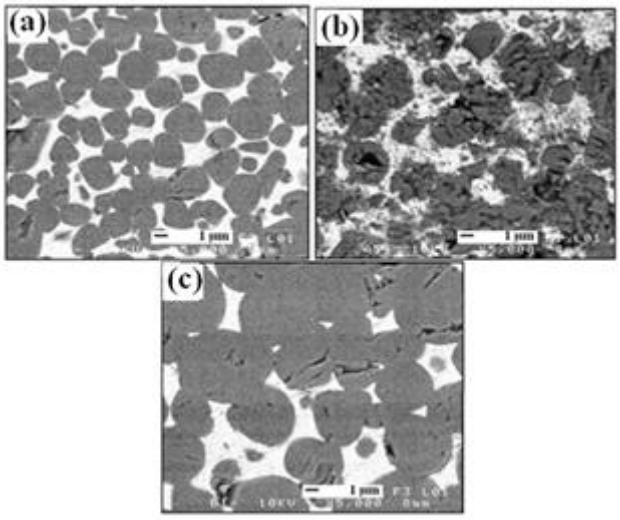

diameter of approximately 2 μm (Table 4) surrounded by the metallic binder. This microstructure contrasts with that of sample S_{01} (Fig. (4b)), in which the TiC particles are characterized by an intense cracking. The application of load throughout the whole process generates a highly disturbed structure, thus making the TE/HP procedure inefficient.

The Cr addition to the starting mixture (S_1 sample) caused significant changes in the microstructure of the TiC-Ni based cermet (Fig. (4c)). A notable grain growth of TiC particles was observed when compared with S_0 cermet. SEM observation associated with EDS analysis (Fig. 5) confirmed that the S_1 cermet consisted of three distinct phases: spherical TiC particles, 4.65 μm on average (Table 4), surrounded by the binder phase, with most of the Cr concentrated in regions, randomly distributed within the metal binder. EDS analyses performed in these Cr-rich regions showed a Cr content exceeding 50 at.% (Fig. (5a) and (5b),

Figure 5. SEM micrograph (a) and EDS analysis results (a, b) of S_1 cermet containing Cr.

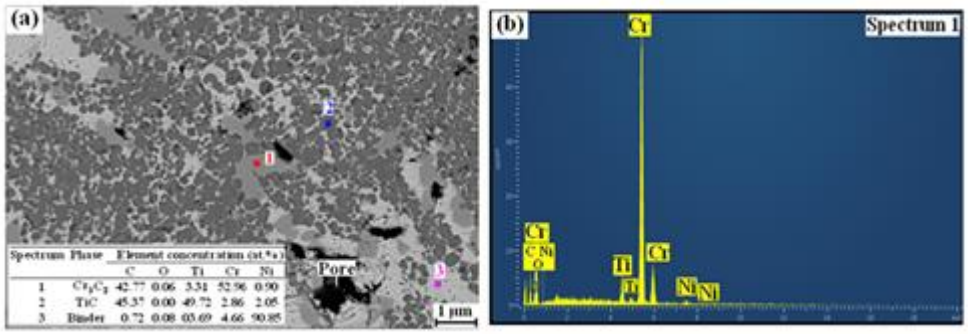

spot spectrum 1) and was associated with the presence of Cr_3C_2 carbide. Remember that this phase was identified in the XRD pattern (Fig. 2). EDS analysis confirmed that the metal binder consisted mainly of Ni with low contents of Cr and Ti, which were dissolved in the transient liquid phase formed during the thermal explosion process (spot 3). In this cermet, the core-rim structure was not observed in agreement with the literature results.

The addition of Mo to the initial mixture was also responsible for notable changes in the TiC-Ni based cermet microstructure, as perfectly illustrated by the SEM micrograph of S_2 sample (Fig. 6(a)). In this case, the core-rim structure was observed and TiC particles adopted several morphologies. Moreover, a finer microstructure was obtained, with a mean particle size of 1.80 µm (Table 4). Two main types of TiC particles could be identified. Type A particles have a core-rim structure in which the dark central part occupies most of the particle and is surrounded by a thin rim. However, in type B particles, the rim is larger than the core and comprises several rim layers with different contrasts (Fig. 6(a)).

EDS analyses carried out along the radius of a spherical TiC particle (type B) permitted to identify at least three distinct zones in the core-rim structure (Figs. 6 (a), (b)). They all consist of complex (Ti, Mo)C carbides with variable molybdenum contents. In this case, the inner rim is more developed (inset in Fig. (6a)) and is characterized by the highest Mo content (25 wt.%), which explains its brighter appearance compared to the core and the outer rim. For

their part, the core and the outer rim have more similar compositions, but the core possesses the highest Ti content.

Figure 6. SEM micrograph (a) and EDS analyses results (b) of S_2 cermet containing Mo after the TE + HP procedure. SEM micrograph of S'_2 cermet after TE procedure (c).

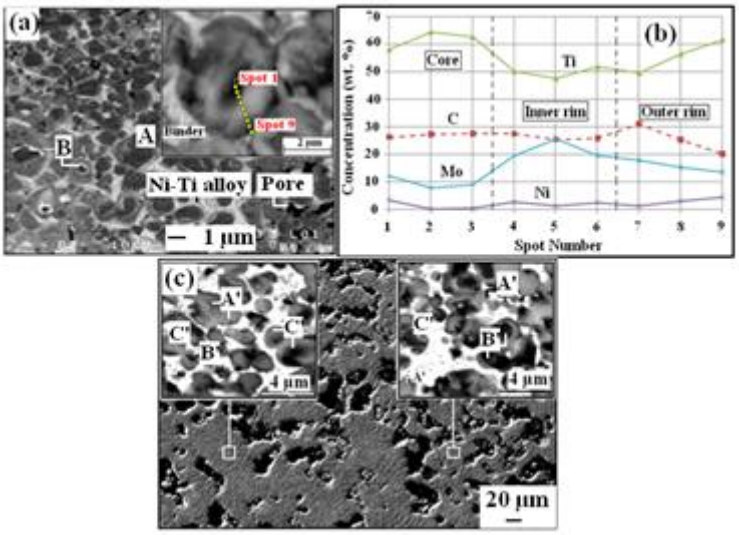

Note that the core, which is the undissolved original particle, is also a mixed (Ti, Mo)C carbide that confirms the formation of this solid solution during the thermal explosion synthesis.

For a better understanding of the core-rim structure evolution during the TE + HP procedure, several samples were also subjected to a thermal explosion process without post-isothermal dwelling (TE procedure). Figure 6(c) shows the microstructure of S'_2 sample with Mo (Table 3) obtained according to this regime. A high porosity was observed that is characteristic, as mentioned before, of samples produced by combustion from reactive mixtures. SEM observations under high magnification highlighted some interesting differences in the microstructure compared to the S_2 cermet. In the S'_2 cermet, the microstructure was heterogeneous with a core-rim structure no well-defined and incomplete and with TiC-based particles with many different morphologies. Particles without the core-rim structure were predominant (type A'). These particles constitute in fact the precursors of

the black cores observed in S_2 cermets. There were also fewer particles with an already developed core-rim structure (type B'), whereas other particles (type C') appear to have an incomplete morphology, showing a core often randomly placed in the particle, not in the center. In summary, it can be retain that during the thermal explosion there was not enough time to produce a homogeneous microstructure in the cermet. Taking into account that the solubility of carbides in the binder depends not only on the nature of the heavy element, but also on the temperature, the composition of the reprecipitated carbides should vary according to the temperature profile followed by the sample. The particles with multiple rim layers observed in S_2 cermet should then correspond to the B' and C' particles in S'_2 on which a new rim layer reprecipitates after the isothermal dwelling.

The effects of the W addition in the starting mixture were revealed by the SEM characterization of S_3 sample (Fig. 7(a)). Compared with the S_0 basic sample, the carbide particles retained the spherical shape. In this case, the microstructure was also finer, with a particle size similar to the S_2 sample containing Mo (Table 4).

Figure 7. SEM micrograph (a) and EDS analyses results (b) of S_3 cermet containing W.

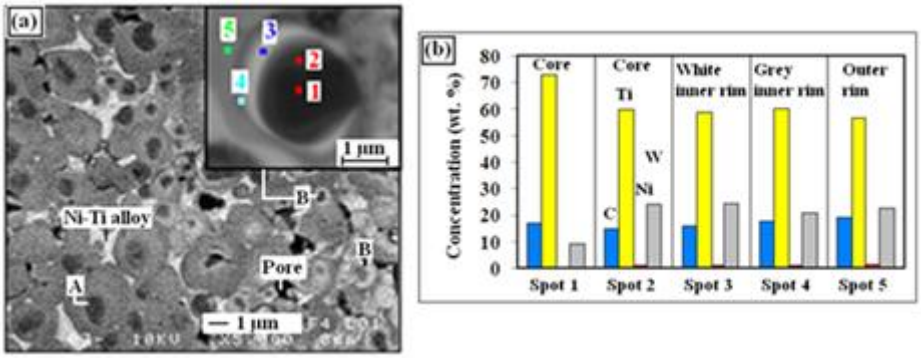

The formation of the core-rim structure seems to inhibit the coarsening of the ceramic particles. These particles had two different appearances (labeled as A and B in Fig. (7a)). The A-type particles had a core-rim structure, in which the core again consists of mixed carbide

(Ti, W)C with a low tungsten content. As in the previous case, the composition of the core confirms that a solid solution was formed during the thermal explosion synthesis. The B-type particles were characterized by the presence of multiple rims around the core. These several rims, with the same (Ti, W)C structure, differed in terms of W content as inferred by the different brightness observed in the SEM micrograph. The minimum W amount (8% wt.) was recorded in the center of the core (Fig. 7, spot 1); although in the periphery a high content exceeding 20% wt. was observed (Fig. 7, spot 2). Spots 3, 4 and 5 illustrate different types of rims (Fig. 7), in which the W content differed slightly with values ranging from 23 to 20 wt.%. Again, the formation of these multiple rims follows a similar mechanism as for cermets containing Mo.

However, as shown in previous work [32], the mechanism of carbides dissolution-reprecipitation in the metallic matrix, on which are based the explanation of the core rim structure formation, can be confirmed by undertaking further sintering kinetics studies of TiC-Ni based cermets.

In summary, the XRD and SEM results allowed the establishment of a probable mechanism governing the formation of the core-rim structure in TiC-Ni-Mo(W) cermets during the TE + HP procedure. In Figure 8, a detailed illustration of this mechanism is given

Figure 8. Schematic illustration of the mechanism governing the core-rim structure formation in cermets obtained by the TE + HP procedure.

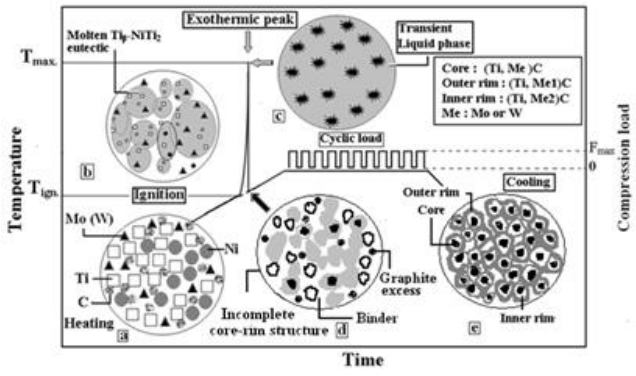

After the cold compaction of the reactive powder mixtures [Ti-C-Ni-Mo(W)] **(a)**, the heating of the sample leads to the formation of the Ti_{β}-$NiTi_2$ eutectic liquid **(b)**. The nucleation and formation of the first TiC particles into this liquid phase that is a strongly exothermic reaction induces the ignition of the sample illustrated by an abrupt increase of the temperature **(c)**. The instantaneous conversion of reactants into TiC promotes the incorporation of Mo or W atoms into the cubic structure to form complex carbides [Ti, Mo(W)]C. At the same time, due to the heat excess of the TiC synthesis reaction, the formation of secondary carbides, Mo_2C or W_2C, also occurs. The dissolution of [Ti, Mo(W)]C and Mo_2C (W_2C) fine particles in the transient liquid phase formed, followed by reprecipitation on the large undissolved particles as the temperature is reduced, involves the appearance of some particles with partial core-rim morphology. Because of the TE process is too fast, the formation of the conventional cermets structure remains heterogeneous and incomplete **(d)**. The final densification and well developed core-rim structure takes place during the dwelling step, which is also characterized by dissolution-reprecipitation transformations, thereby generating a structure consisting of particles having in some cases multiple rim layers **(e)**.

4. Conclusions

This work was dedicated to the study of the development of the core-rim structure in TiC-Ni-based complex cermets obtained by thermal explosion followed by hot pressing under cyclic load. The following conclusions can be drawn:

1-Although T_{ad}, and then $T_{max.}$ reached during the thermal explosion process, depends on the Cr, Mo or W additions, the effects of these additions on $T_{ign.}$ was practically inexistent as $T_{ign.}$ is determined by the appearance of the first liquid phase according to the Ti-Ni phase diagram. However, $T_{ign.}$ decreases when the metal binder content increases as

consequence of the formation of a greater proportion of liquid phase that favors the nucleation of the first TiC particles, inducing ignition.

2- The core-rim structure was only developed in cermets containing Mo or W. The core in these cermets consists of complex carbides, (Ti, Mo)C or (Ti, W)C, since some Mo or W atoms were incorporated to the TiC structure during the synthesis by thermal explosion. The rim, formed by a dissolution-reprecipitation process, is also composed of mixed carbides (Ti, Mo)C or (Ti, W)C, but with a higher content of heavy metals.

3- The formation of the core-rim structure is governed by two different dissolution-reprecipitation processes. The first one is very fast and occurs by the dissolution of carbide fine particles in the transient liquid phase formed during the exothermic peak, followed by a reprecipitation on the undissolved particles. In this case, the structure remains incomplete and heterogeneous. The second process takes place during the isothermal dwelling. These two processes with different temperature and time scales give result in the formation of particles with multiple rim layers.

4- The core-rim structure generates in the TiC particle a strain state which evolves as a function of additions nature and applied regime.

5-The Cr addition did not create the core-rim structure, but induced a notable TiC particle coarsening. The appearance of the core-rim structure with Mo or W addition substantially inhibited the grain growth. Unfortunately, regarding the residual porosity, the opposite effect was observed. In presence of Mo or W, the cermet had a lower relative density. Nevertheless, the highest hardness value (18000 MPa) was recorded for the TiC-Ni cermet containing Mo. Hardness was 16320 MPa and 15110 MPa for cermets with W and Cr additions, respectively.

Acknowledgements

The authors sincerely thank Professor M. Benabdeslem of LESIMS Laboratory - Department of Physics, Annaba University for its assistance in carrying out the XRD analyses.

References

[1] P. Ettmayer, H. Kolaska, W. Lengauer, K. Dreyer, Ti(C,N) Cermets-metallurgy and properties, Int. J. Refract. Met. Hard Mater 13 (1995) 343-351.

[2] S. Cardinal, A. Malchère, V. Garnier, G. Fantozzi, Microstructure and mechanical properties of TiC–TiN based cermets for tools application, Int. J. Refract. Met. Hard Mater 27 (2009) 521–527.

[3] A. Rajabi, M.J. Ghazali, J. Syarif, A.R. Daud, Development and application of tool wear: A review of the characterization of TiC-based cermets with different binders, Chem. Eng. J. 255 (2014) 445–452.

[4] X. Ren, H. Miao, Z. Peng, A review of cemented carbides for rock drilling: An old but still tough challenge in geo-engineering, Int. J. Refract. Met. Hard Mater 39 (2013) 61–77.

[5] N. Liu, S. Chao, H.D. Yang, Cutting performances, mechanical property and microstructure of ultra-fine grade Ti(C,N)-based cermets, Int. J. Refract. Met. Hard Mater 24 (2006) 445–52.

[6] L.M. Chen, W. Lengauer, P. Ettmayer, K. Dreyer, H.W. Daub, D. Kassel, Fundamentals of liquid phase sintering for modern cermets and functionally graded cemented carbonitrides (FGCC), Int. J. Refract. Met. Hard Mater 18 (2000) 307-322.

[7] S.Y. Ahn, S. Kang, Formation of core/rim structures in Ti(C,N)-WC-Ni cermets via a dissolution and precipitation process, J. Am. Ceram. Soc. 83 (2000) 1489-94.

[8] P. Li, J. Ye, Y. Liu, D. Yang, H. Yu, Study on the formation of core rim structure in Ti(C, N)-based cermets, Int. J. Refract. Met. Hard Mat 35 (2012) 27–31.

[9] Q. Yang, W. Xiong, S. Li, J. Li, Effect of partial substitution of Cr for Ni on densification behavior microstructure evolution and mechanical properties of Ti(C, N)–Ni-based cermets, J. Alloys Compd. 509 (2011) 4828–34.

[10] Y. Li, N. Liu, X. Zhang, C. Rong, Effect of Mo addition on the microstructure and mechanical properties of ultra-fine grade TiC–TiN–WC–Mo_2C–Co cermets, Int. J. Refract. Met. Hard Mater 26 (2008) 190–96.

[11] H.O. Andrén, Microstructures of cemented carbides, Mater. Des. 22 (2001) 491-8.

[12] O. Kruse, B. Janson, K. Frisk, Experimental study of invariant equilibria in the Co-W-C and W-C-M (M= Ti, Ta, Nb) systems, J. Phase Equilib. 22 (2001) 552-5.

[13] S. Kang, Cermets, In Vinid K. Sarin, editor, Comprehensive Hard Materials.vol.1, Elsevier, 2014, 139-81.

[14] Y. Peng, H. Miao, Z. Peng, Development of TiCN-based cermets: mechanical properties and wear mechanism, Int. J. Refract. Met. Hard Mat 39 (2013) 78–89.

[15] E. Chicardi, J.M. Cordoba, M.J. Sayagués, F.J. Gotor, Absence of the core-rim microstructure in $Ti_xTa_{1-x}C_yN_{1-Y}$ based cermets developed from a pre-sintered carbonitride master alloy, Int. J. Refract. Met. Hard Mat. 33 (2012) 38–43.

[16] A. Rajabi, M.J. Ghazali, A.R. Daud, Chemical composition, microstructure and sintering temperature modifications on mechanical properties of TiC-based cermet–A review, Mater. Des. 67 (2015) 95–106.

[17] G. Liu, J. Li, K. Chen, Combustion synthesis of refractory and hard materials: A review, Int. J. Refract. Met. Hard Mat. 39 (2013) 90–102.

[18] G. Xiao, Q. Fan, M. Gu, Z. Wang, Z. Jin, Dissolution-precipitation mechanism of self-propagating high-temperature synthesis of TiC-Ni cermet, Mat. Sci. Eng. A 382 (2004) 132–40.

[19] Y.F. Yang, H.Y. Wang, R.Y. Zhao, Y.H. Liang, L. Zhan, Q.C. Jiang, Effects of C particle size on the ignition and combustion characteristics of the SHS reaction in the 20 wt.% Ni–Ti–C system, J. Alloys Compd. 460 (2008) 276–82.

[20] H. Boutefnouchet, C. Curfs, A. Triki, A. Boutefnouchet, D. Vrel, Self-propagating high-temperature synthesis mechanisms within the Ti–C–Ni system: A time resolved X-ray diffraction study, Powder Technol. 217 (2012) 443–50.

[21] A. Azadmehr, E. Taheri-Nassaj, An in situ (W, Ti)C–Ni composite fabricated by SHS method, J. Non-Cryst. Solids 354 (2008) 3225–34.

[22] X. Chen, W. Xiong, Z. Yao, G. Zhang, S. Chen, Q. Yang, A characterization of Ti-based solid solution cermets prepared by mechanically induced self-sustained reaction and subsequent pressureless sintering, J. Alloys Compd. 583 (2014) 523–9.

[23] E. Chicardi, F.J. Gotor, V. Medri, S. Guicciardi, S. Lascano, J.M. Cordoba, Hot pressing of (Ti, Mt)(C, N)-Co-Mo_2C (Mt=Ta, Nb) powdered cermets synthesized by mechanically induced self-sustaining reaction, Chem. Eng. J. 292 (2016) 51-61.

[24] S. Boudebane, S. Lemboub, S. Graini, A. Boudebane, A. Khettache, J. Le Lannic, Effect of binder content on relative density, microstructure and properties of complex cemented carbides obtained by thermal explosion-pressing, J. Alloys Compd. 487 (2009) 235–42.

[25] E.R. Strutt, E.A. Olevsky, M.A. Meyers, Combustion synthesis quasi-isostatic pressing of TiC-NiTi cermets: processing and mechanical response, J. Mat. Sci. 43 (2008) 6513–26.

[26] H. Jie-Cai, X.H. Zhang, J.V. Wood, In-situ combustion synthesis and densification of TiC–xNi cermets, Mat. Sci. Eng. A 280 (2000) 328–33.

[27] G.K. Williamson, W.H. Hall, Author links open the author workspace. X-ray line broadening from filed aluminum and wolfram, Acta Metall. 1 (1953) 22-31.

[28] H. Pierson, Handbook of Refractory Carbides and Nitrides—Properties, Characteristics, Processing and applications, Noyes Publications Westwood, NJ, (1996).

[29] B. Holt, Z.A. Munir, Combustion synthesis of titanium carbide: Theory and experiment, J. Mat. Sci. 21 (1986) 251-9.

[30] K. Morsi, The diversity of combustion synthesis processing: a review, J. Mater. Sci. 47 (2012) 68–92.

[31] A.I. Gusev, A.A. Rempel, A.J. Magerl, Disorder and order in strongly nonstoichiometric compounds: Transition Metal Carbides, Nitrides and Oxides. Springer-Verlag Berlin Heidelberg; 2001.

[32] J.D. Bolton, A.J. Gant, Microstructural development and sintering kinetics in ceramic reinforced high speed steel metal matrix composites, Powder Metall. 40 (1997) 143-151.

Highlights

- The structure of TiC-Ni based cermets containing Mo or W obtained by thermal explosion (TE) and hot-pressing (HP) shows specific core-rim structure constituted by mixed carbides (Ti, Mo)C or (Ti, W)C with different contents of heavy metal.
- The cermets structure formation is governed by two dissolution-reprecipitation mechanisms first, in the transient liquid phase during exothermic peak and second, in solid phase during isothermal dwell
- After TE process, the formation of the conventional core-rim structure remains heterogeneous and incomplete.
- The final densification and well developed core-rim structure is obtained after (TE + HP) regime and the structure is formed of particles with multiple rim layers.
- The core rim structure generates in the TiC particle a strain state which evolves as a function of additions nature and applied regime.